Biomedical Paper

A Six-Degree-of-Freedom Passive Arm with Dynamic Constraints (PADyC) for Cardiac Surgery Application: Preliminary Experiments

Olivier Schneider, Ph.D., and Jocelyne Troccaz, Ph.D.
Laboratoire TIMC/IMAG, Faculté de Médecine, Université Joseph Fourier, La Tronche, France

ABSTRACT The purpose of Computer-Assisted Surgery (CAS) is to help physicians and surgeons plan and execute optimal strategies from multimodal image data. The execution of such planned strategies may be assisted by guidance systems. Some of these systems, called synergistic systems, are based on the cooperation of a robotic device with a human operator. We have developed such a synergistic device: PADyC (Passive Arm with Dynamic Constraints). The basic principle of PADyC is to have a manually actuated arm that dynamically constrains the authorized motions of the surgical tool held by the human operator during a planned task. Dynamic constraints are computed from the task definition, and are implemented by a patented mechanical system. In this paper, we first introduce synergistic systems and then focus on modeling and algorithmic issues related to the dynamic constraints. Finally, we describe a 6-degree-of-freedom prototype robot designed for a clinical application (cardiac surgery) and report on preliminary experiments to date. The experimental results are then discussed, and future work is proposed. Comp Aid Surg 6:340–351 (2001). ©2002 Wiley-Liss, Inc.

Key words: **medical robotics, man/robot cooperation, cardiac surgery, synergistic devices, computer-assisted surgery**

INTRODUCTION

Over the last 2 decades, medical robotics has evolved from the adaptation of industrial robots to medical tasks to a specific domain of robotics requiring the development of innovative architectures and control modes. Classical taxonomies distinguish three types of guidance systems for computer-aided surgery: active, passive, and semiactive systems. In this division, the degree of passivity corresponds to the type of interaction between the human and the device.

1. Passive systems display information to the surgeon about the position of the surgical tool relative to anatomical data or to a preplanned strategy, but the surgeon is totally responsible for the execution of the surgical action. Such a system is generally based on the use of a localizer (an encoded mechanical arm or a device based on optical, magnetic, or ultrasonic technologies), which tracks the surgical instrument and other ob-

Address correspondence/reprint requests to: Jocelyne Troccaz, Ph.D., Laboratoire TIMC/IMAG, Faculté de Médecine, Domaine de la Merci, F-38706 La Tronche cedex, France; Telephone: +33 (0)4 76 54 95 08; Fax: +33 (0)4 76 54 95 55; E-mail: jocelyne.troccaz@imag.fr.

Published online in Wiley InterScience (www.interscience.wiley.com). DOI: 10.1002/igs.10020

jects of interest. References 1–3 present typical examples of passive systems.

2. Active systems realize a part of the intervention autonomously. A robot may machine a bone, or hold a sensor or surgical tool, without the need for interaction with the human operator, who generally supervises the action. For examples, see refs. 4 and 5.
3. A semiactive system involves a combined action with the human operator for the complete realization of the task. For example, a mechanical guide positioned by a robot[6,7] or manually[8,9] may align a linear drilling trajectory that the surgeon then executes.

This classification has some limitations. Robotic systems for telesurgery (such as that described by Guthart and Salisbury[10]) are somewhat difficult to classify in these three categories because the master and slave manipulators involve different types of interaction. Moreover, the precise meaning of "semiactive" is quite variable in the community. Nevertheless, this existing classification is well known, and constitutes a good basis for discussion.

Each of these systems has its own advantages and drawbacks, and the selection of which one to use is highly dependent on the application needs.[11] Because our goal is to develop robotic systems that enable tight cooperation between man and machine, we focused on semiactive systems. These allow an ergonomic, direct, and accurate transfer of the surgical planning to the operating site. Nevertheless, they are restricted to rather elementary tasks such as linear motions and planar cuts. Moreover, this transfer is implemented using task-specific hardware; this hardware may be considered as the implementation of a *mechanical constraint.* Such mechanical constraints need to be generalized and made programmable. Therefore, we proposed the new concept of *synergistic devices.* Synergistic devices are intended for direct physical guidance of a surgical tool, a tool that is also held and controlled directly by a surgeon. The concrete objective is to build general-purpose mechanical devices designed to be held in the surgeon's hand, allowing him to feel the virtual world of patient data (including safety regions around anatomical obstacles that are to be avoided) and surgical strategies while moving in the real world.

PRINCIPLES

Basic Principle of the Synergy

The basic principle of these devices is as follows. Both the surgeon and the synergistic device hold the tool, apply forces to it and to each other, and impart motions. Under computer control, the synergistic device may allow the surgeon to have control of some degrees of freedom (DOF) while the device controls the others. The system filters the motions proposed by the surgeon, keeping only those that are compatible with the surgical plan (see Fig. 1). For instance, during the preplanning stage, an orthopedic surgeon selects a cutting plane for machining a bone before implanting a knee prosthesis. In such a case, the synergistic system guarantees that the motions of the cutting tool are strictly limited to the preplanned plane, while the surgeon is in charge of the selection of motions within the plane. Such a system takes the best advantage of (1) the robot and its computer-based model of the surgical action, and (2) the surgeon and his knowledge, sensing capabilities, and ability to react to unexpected or nonmodeled events.

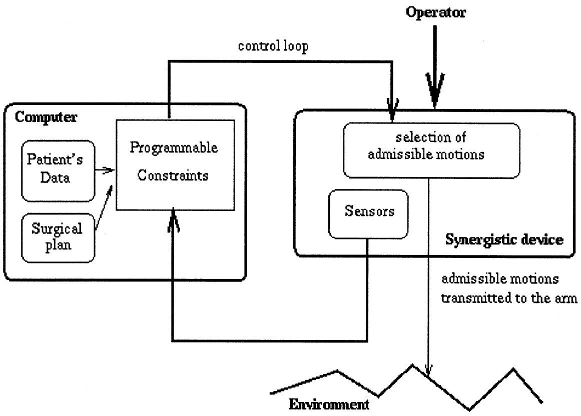

Fig. 1. General principle of the PADyC system.

The principle of synergy is rather recent, although a somewhat similar system was proposed by Taylor et al.[12] to improve the usability of a passive mechanical arm by means of particle brakes. Synergistic systems have been implemented using several types of technologies. Acrobot (Active Constraint Robot), an implicit force-controlled robot, is used for knee surgery.[13,14] The surgeon guides the bone cutter while Acrobot guarantees that the tool remains in the planned region. The system helps the surgeon by restraining his ability to move towards the forbidden region by progressively increasing the resistance of the motors. The motors and the operator are considered at the same level in the control loop. Burghart et al.[15] developed a similar approach using a force-controlled robot for craniofacial surgery. Whereas these two systems are based on an active mecha-

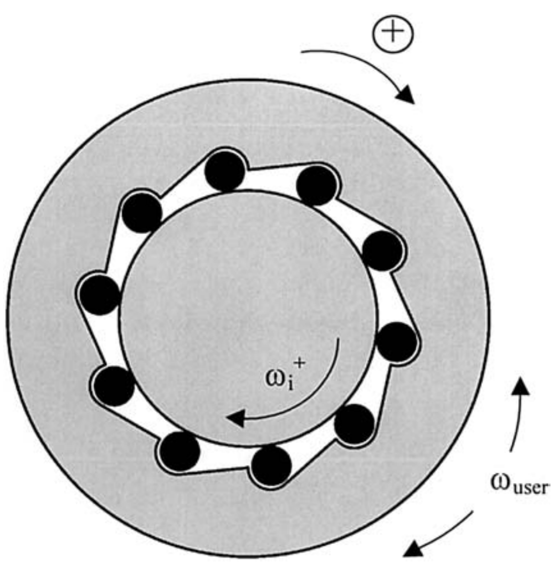

Fig. 2. Freewheel mechanism.

nism, P-TER,[16] Cobot[17,18] and PADyC are based on passive joints. Cobot (Cooperative robot) is based on nonholonomic elements allowing the coupling of DOFs. For instance, for a planar 3DOF (two translations and one rotation) Cobot, x, y, and α parameters are defined such that tg α = vy/vx, where vx and vy are the Cartesian velocities in the plane of motion. PADyC's principles were introduced in ref. 19. The system is presented in full detail in the following sections.

Mechanical Architecture of a Single Joint

To constrain the motion of the end-effector in the performance of a given task, each joint of the PADyC has to be able to provide the four following functions: (1) F1: motion authorized in the positive direction only; (2) F2: motion authorized in the negative direction only; (3) F3: motion authorized in both directions; and (4) F4: no motion authorized.

These four functions are provided using a patented mechanism associated with each encoded joint. The mechanism consists of two freewheels mounted in opposite directions and associated with two motors. A freewheel is very similar to a conventional roller bearing, but it naturally provides the basic function of unidirectional motion. For instance, as shown in Figure 2, let us consider that the internal part of the freewheel is fixed ($\omega_i^+ = 0$). If the operator imparts motion to the external part of the freewheel with velocity ω_{user} in the positive direction, the motion will be blocked while the motion is free in the negative direction. If a motor is now associated with the internal part of the freewheel and rotates with velocity ω_i^+, then both directions of motion are allowed but ω_{user} is bounded by ω_i^+ in the positive direction.

For one joint, each of the two freewheels is associated with one clutching motor rotating in a single direction. The velocities ω_i^- and ω_i^+ of the two motors associated with the joint J_i are computer controlled. The operator moves the other part of the freewheel at velocity ω_{user}. Depending on the values of the relative velocities ($\omega_i^{+,-} - \omega_{\text{user}}$), the motion is blocked or authorized. Based on this mechanism, one can guarantee that, at each instant, the resulting velocity ω_i of the joint J_i is bounded by $\omega_i^- \leq \omega_i \leq \omega_i^+$.

This mechanism allows us to clutch or declutch the freewheels and to obtain the four functions F1 to F4 by a suitable choice of the $\omega_i^{+,-}$ values:

$$\text{F1: } \omega_\text{i}^- = 0 \wedge \omega_\text{i}^+ \leq 0$$

$$\text{F2: } \omega_\text{i}^- \leq 0 \wedge \omega_\text{i}^+ = 0$$

$$\text{F3: } \omega_\text{i}^- \leq 0 \wedge \omega_\text{i}^+ \leq 0$$

$$\text{F4: } \omega_\text{i}^- = 0 \wedge \omega_\text{i}^+ = 0$$

The intrinsic safety of such a system is good. Indeed, the joint mechanical design integrates another set of freewheels and worm screws that respectively guarantee that the arm cannot move autonomously, because the motors cannot drive the joints, and that the user cannot back-drive the motors. Moreover, the joints are naturally locked when unpowered.

Task and Dynamic Constraints

A surgical strategy is defined in terms of "task constraints." These constraints are generally defined in the Cartesian space from multimodality patient data. Examples include a trajectory that has to be executed relative to a given anatomical structure, or a surgical tool that has to explore a predefined space while avoiding organs at risk. These constraints apply to one or several control points positioned on the surgical tool or on the synergistic device. We have defined four programming modes corresponding to basic types of task constraints:

1. *Free mode*. In this mode, PADyC behaves as a mechanical localizer. No specific constraint applies. The position of the surgical tool is computed and recorded.
2. *Position mode*. PADyC helps the user to move the tool towards a predefined position

and orientation. For instance, a bone fragment or a prosthesis component may be positioned relative to bony structures according to a preplanning step.

3. *Trajectory mode.* This mode constrains the motion to follow a predefined trajectory with a given accuracy. A biopsy trajectory, for example, will be executed in this way.
4. *Region mode.* The tool is free to move in a given region of space, but cannot escape from that region. Motion inside the region is totally free and unconstrained. This allows a surgeon to stay in a region to remove some tissue (e.g., tumor resection or cavity preparation for prosthesis placement) or to guarantee that some critical structures will be avoided.

More specialized modes have been defined: linear trajectory motion, planar region motion, and conical region motion. Combined modes can also be defined; for example, a position has to be reached while avoiding structures at risk.

The task is described in terms of these programming modes. Such a description may be generated from the planning tools included in classical CAS systems. For example, the shape of a 3D region in which the tool must remain is computed from anatomical data of the patient obtained before the intervention. In such a case, the 3D representation of the region is the main parameter of the mode.

A second set of constraints called "dynamic constraints" results from the integration by the system of the task constraints and the current configuration of the synergistic system. They are computed such that, at each instant, task constraints are satisfied. The representation of dynamic constraints depends on the synergistic system. In the case of Cobot, for example, a dynamic constraint is an equation connecting joint variables. Because the PADyC joint mechanism has been designed so that each joint velocity can be constrained in both direction and amplitude, dynamic constraints correspond to velocity orders. The high-level control of PADyC is in charge of the translation of task constraints to dynamic constraints. The following sections describe these algorithms.

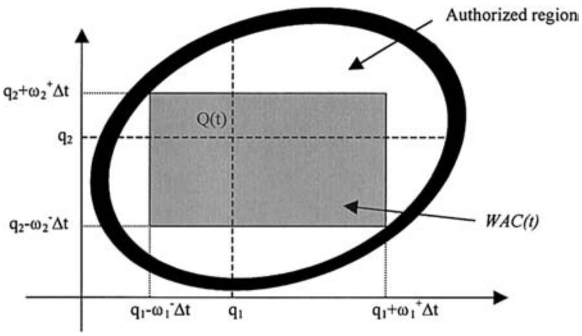

Fig. 3. Window of admissible configurations (a simple example).

Modeling the Dynamic Constraints

As presented below, at each instant, each joint is constrained to move in a given direction with a bounded amplitude. The velocity window $[\omega_i^-, \omega_i^+]$ associated with each joint J_i guarantees that, during the next sampling period Δt, the configuration of the robot belongs to a known hyper-parallelepiped parallel to the joint axes, called the *window of admissible configurations* or WAC (see Fig. 3). (In the following, for the sake of readability, illustrations will correspond to the case of a 2DOF PADyC.) For an n-joint robot, the WAC is defined as WAC(t) $= (\Delta q_1^-, \Delta q_1^+, \Delta q_2^-, \Delta q_2^+, \ldots, \Delta q_n^-, \Delta q_n^+)$.

The constraint executed at instant t and available until $t + \Delta t$ may be described by the dynamic constraint vector $\Pi(t) = (\omega_1^-, \omega_1^+, \omega_2^-, \omega_2^+, \ldots, \omega_n^-, \omega_n^+)$, where $\omega_i^{-,+}$ are the velocity orders to be sent to the clutching motors of the joint J_i. The major control issue of PADyC concerns the determination, from the current configuration of the robot and the preplanned task, of the vector of dynamic constraint $\Pi(t)$ that has to be applied during the next sampling period to guarantee correct execution of the task. This necessitates computation of the WAC(t), from which $\Pi(t)$ is very easily deduced: $\Pi(t) = \text{WAC}(t)/\Delta t$.

COMPUTING THE DYNAMIC CONSTRAINTS

The low-level control of PADyC is very simple, because it relies on the execution of the velocity orders sent to the motors. Meanwhile, its high-level control requires a mapping of the geometric description of the task from the Cartesian space where it is generally defined to the joint space where the constraints apply (see Fig. 4). This is a very well-known problem of robot motion planning for which computational complexity is a critical issue. Moreover, in our application, the task may vary with time in some cases. For instance, a drilling trajectory in a vertebra will move as a function of the motions of this vertebra during surgery. Therefore, the computational cost of the algorithms used to

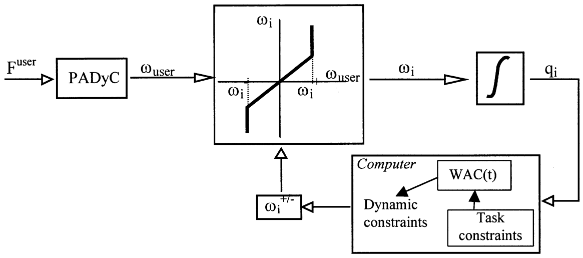

Fig. 4. PADyC control.

map the Cartesian space to the joint space must be kept sufficiently low to allow real-time control. In the following, we introduce the principle of these algorithms for the position and region modes. The free mode control is rather trivial; the trajectory mode may be implemented either as a succession of position modes or as a region mode, which is built from the planned trajectory and its associated tolerance.

Position Mode

Let us consider, for instance, that a configuration $Q^f = (q_1^f, q_2^f, \ldots, q_n^f)$ has to be reached in the position mode, and that $Q^c = (q_1^c, q_2^c, \ldots, q_n^c)$ is the current configuration at the instant t. To help the user to reach Q^f, WAC(t) is defined in the following way (see Fig. 5):

$$\text{if } \mathrm{q}_\mathrm{i}^\mathrm{f} - \mathrm{q}_\mathrm{i}^\mathrm{c} > 0 \text{ then } \Delta\mathrm{q}_\mathrm{i}^- = 0 \text{ and } \Delta\mathrm{q}_\mathrm{i}^+ = \mathrm{q}_\mathrm{i}^\mathrm{f} - \mathrm{q}_\mathrm{i}^\mathrm{c}$$

$$\text{else } \Delta\mathrm{q}_\mathrm{i}^- = \mathrm{q}_\mathrm{i}^\mathrm{f} - \mathrm{q}_\mathrm{i}^\mathrm{c} \text{ and } \Delta\mathrm{q}_\mathrm{i}^+ = 0$$

In this way, at each sampling period, the current configuration is closer to the goal configuration.

Region Mode

As already stated, computing WAC(t) is more difficult for trajectories or regions. A major difficulty lies in representing in the joint space an object—for example, a region—defined in the Cartesian space. The region may be, for example, the shape of a cavity to be machined with the surgical tool. To avoid this computation, we developed an approach inspired by the work of Barraquand and Latombe.[20] It consists of replacing this 6D problem, i.e., computing the region in the joint space and deducing the range of available positions and orientations of the surgical tool, by the combination of several much simpler 3D problems: computing available positions of a set of k control points Pj located on this tool. Thus, for each of the k control points Pj, a local WAC$_j(t)$ is computed. To compute WAC$_j(t)$ at an instant t, when PADyC is in the configuration Q^c, the position of P_j is evaluated using the robot direct kinematics model. A ball $B_j(t)$ of admissible positions is determined locally in the Cartesian space, using a precomputed 3D chamfer distance map. Then, the algorithm determines a WAC$_j(t)$ whose image in the Cartesian space, called WAC$_j^{\mathrm{cart}}(t)$, is included in the ball $B_j(t)$. To speed up this process, we can use a linear approximation of WAC$_j(t)$ because, as the sampling period Δt is small, $B_j(t)$ is also small. Finally WAC(t) is simply defined as

$$\mathrm{WAC}(t) = \bigcap\nolimits_{j=1}^{k} WAC_j(t)$$

The rationale is that the constraint is globally satisfied if it is locally satisfied by all the control points. As WACs are very simple mathematical objects, their intersection is straightforward.

The specific modes are based on similar approaches, but they allow for more rapid computations than this general algorithm used for free-form regions or trajectories. Finally, the combined modes are implemented as a conjunction of constraints, and therefore equivalently as an intersection of WACs.

For more details about these methods, please refer to refs. 21–23.

IMPLEMENTATION OF PADYC

Previous Prototypes

Several prototypes of PADyC were realized and evaluated. The very first system was a Meccano™ assembly (Fig. 6a), which allowed us to test the basic design idea of a single joint equipped with two freewheels and two clutching motors. The second prototype was a single joint equipped with an encoder and two computer-controlled motors (Fig. 6b). It allowed us to test the basic velocity control

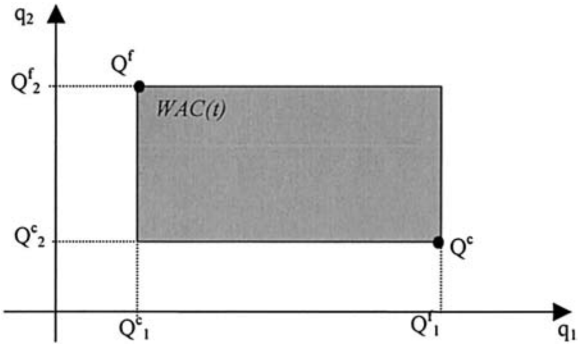

Fig. 5. Position mode: computing WAC(t).

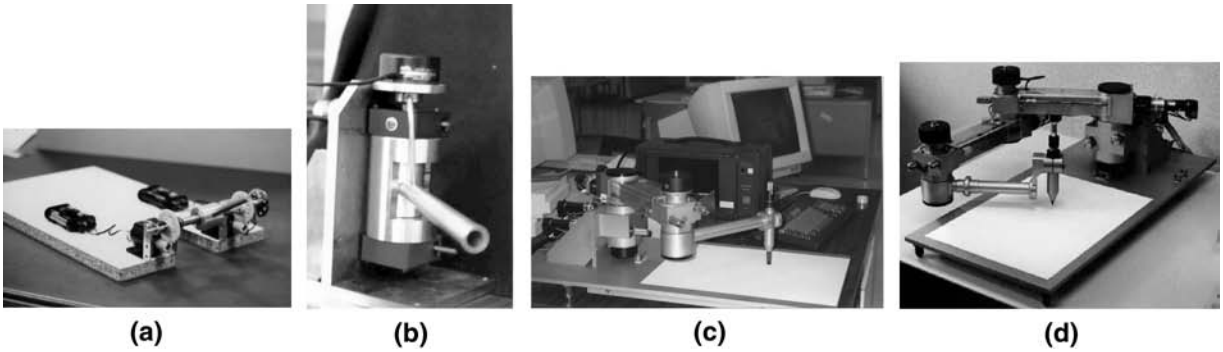

Fig. 6. PADyC prototypes: (a) one axis (uncontrolled), (b) one axis, (c) two axes, (d) three axes. [Color figure can be viewed in the online issue, which is available at www.interscience.wiley.com]

of a single joint. The third system was a planar 2DOF prototype (Fig. 6c). As can be seen in the illustration, the end-effector is a pen, allowing us to visualize executed motions and trajectories. The four basic modes were implemented on this prototype, and successful experiments were run. A third axis was later added to experiment with redundancy (Fig. 6d). These experiments are reported in refs. 21 and 24.

A Six-Degree-of-Freedom Prototype: For What Purpose?

Based on those previous developments, it was decided to develop a 6DOF PADyC on a more clinical basis. We selected one application where neither traditional passive systems nor active robots are fully satisfactory. Pericardial puncture, also called pericardiocentesis, is a task well suited for the clinical evaluation of PADyC. This procedure consists of removing some pathological liquid from the pericardium using a needle. The percutaneous access to the effusion (a subcostal access through the skin) can only be performed when the effusion is large enough, typically more than 15 mm in the direction of motion. This threshold is used to prevent the puncture needle from accidentally damaging the heart. The percutaneous procedure is almost blind for the surgeon, who cannot easily track the needle on intraoperative echographic images. This is one reason why pericardial puncture is a difficult procedure, with a failure rate of 20% and a 5% risk of puncture of the heart, which may lead to the death of the patient.[25] When the effusion is too small for a safe percutaneous access, the cardiac surgeon performs an open procedure, which is very invasive and traumatic. To decrease the threshold of percutaneous puncture while allowing a safe procedure, we developed the CASPER (Computer ASsisted PERicardial puncture) system.[26] CASPER is based on passive optical guidance. After an echographic imaging procedure, a safe target position and a safe trajectory are computed. During surgery, the position of the needle is tracked with the optical localizer and a user interface displays on a computer screen information about the current position and orientation of the needle with respect to the planned path, as shown in Figure 7. Animal experiments[27] have shown that CASPER allows the surgeon to safely puncture much smaller effusions. Although the system increases the accuracy of the procedure, problems remain from an ergonomic point of view. The surgeon felt quite uncomfortable in maintaining a stable trajectory through the different layers of soft tissue while controlling the needle depth on a screen. In this clinical application, the distance of the needle tip to the heart is a critical parameter because the heart must be avoided at all costs. As safety is critical in this application, we preferred to develop a synergistic system such as PADyC rather than introduce an active robot.

In this PADyC-based version of CASPER, the feedback is basically haptic, so the use of a screen is not strictly necessary. This should result in a more comfortable use of the computer data during the intervention and in a more natural action for the surgeon, whose focus should be only on the needle. As a result of better stability in the trajectory, accuracy and system usability should increase.

Architecture of the System

Based on the application specifications, a six-axis SCARA architecture was designed. As can be seen in Figure 8, the PADyC axes are: one vertical translation, three rotations around vertical axes, one rotation around a horizontal axis, a modular sixth joint (see Fig. 8c), which can be either a rotation

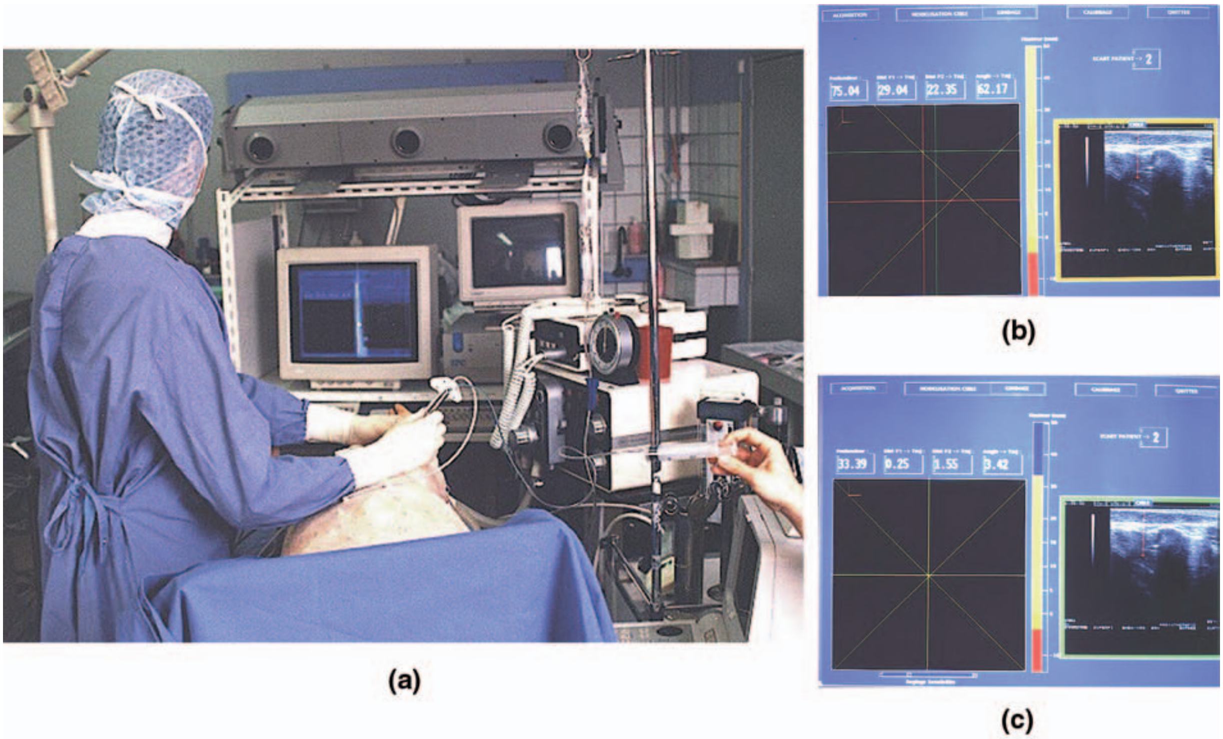

Fig. 7. CASPER navigation system: (a) the guiding system; (b) the display before trajectory alignment; (c) the display during needle progression. [Color figure can be viewed in the online issue, which is available at www.interscience.wiley.com]

axis or a translation axis. Figure 8a and b shows the translation module fixed on the robot.

The first joint is associated with a counterweight to improve the system transparency by decreasing the forces required to move the arm upward. Downward motions are made easier due to gravity. The first three axes are equipped with magnetic brakes. The resulting useful workspace of the end-effector may be approximated by a parallelepiped about 20 cm high with dimensions of 30 × 30 cm.

The control system is implemented on an industrial PC running the real-time operating system QNX. This operating system allows us to guarantee a control loop rate of 100 Hz under any conditions. High-level control algorithms are implemented in the C++ language.

The expected use of the PADyC-based CASPER system is the following. It is very similar to the passive version of CASPER, presented in the previous section, in terms of the surgical protocol. The six-axis device will replace the navigation system (i.e., the optical localizer and the display). In the first stage, the echographic probe is mounted on the rotation module and attached to the robot's end-effector. The probe is used for image acquisition. After the planning phase, where the target position and approach trajectory are defined, the probe module has to be removed from PADyC. The needle is then mounted on the translation module that replaces the rotation module. Then, the surgeon, assisted by the robot, performs the pericardial puncture. First, using the position mode, the needle has to be aligned with the planned trajectory. When the needle is in the correct approach configuration, the first five axes are kept in position, the clutching motors are stopped, and the brakes are activated. Then, using the translation module, the needle progression toward the target point is executed using a position mode on the sixth axis. Because the reverse motion of the needle is not critical, the sixth axis translation module is equipped with a single freewheel and its associated clutching motor. Motion toward the target is velocity controlled; motion backward is free. Moreover, this allows the surgeon to remove the needle very rapidly if a problem arises.

EXPERIMENTS AND PRELIMINARY RESULTS

The system is not yet totally integrated with the application. Nevertheless, a number of tests have been performed to evaluate the basic properties of

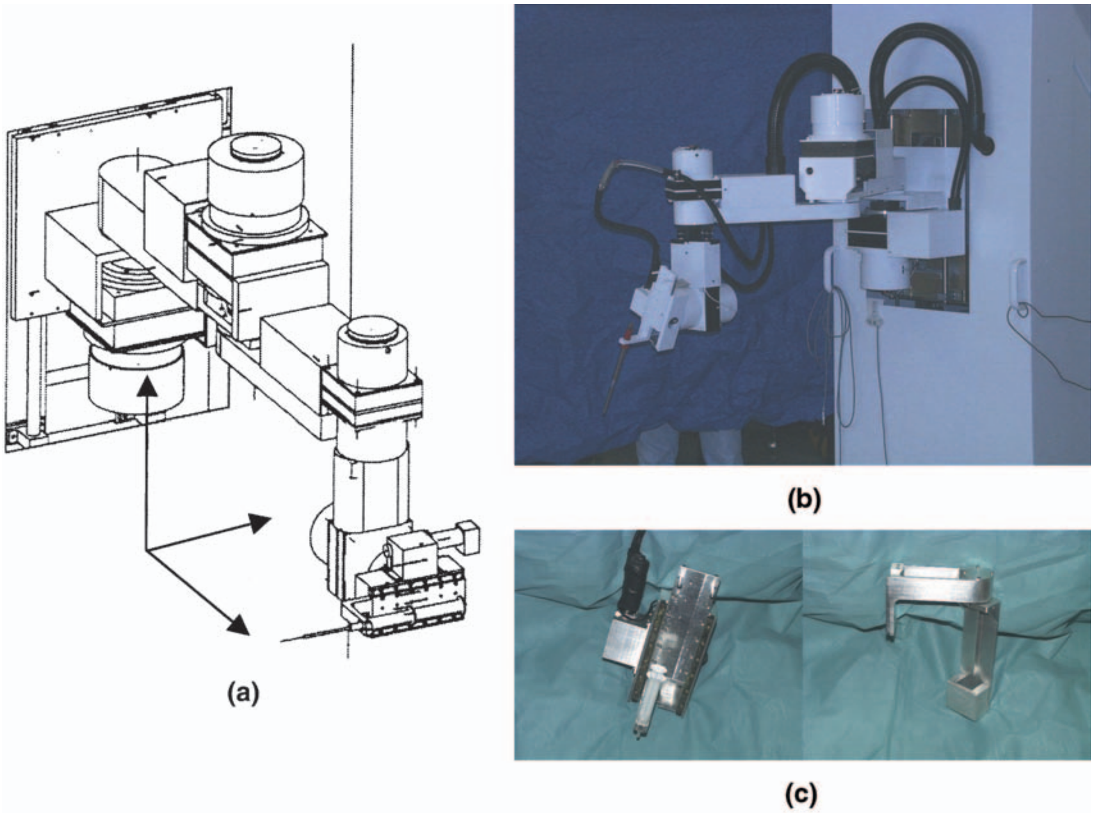

Fig. 8. PADyC 6-axis prototype: (a) general sketch; (b) the prototype; (c) the 6th axis modules (translation or rotation). [Color figure can be viewed in the online issue, which is available at www.interscience.wiley.com]

the arm and the control algorithms. The experiments make use of an external measurement device: a 6D optical localizer (Optotrak™, Northern Digital, Inc., Ontario). Optotrak localizes infrared diodes fixed to moving objects; this allows the tracking of several objects within a measurement volume of 1 m^3 with very good accuracy. [More precisely, several tests (intrinsic accuracy, relative accuracy, etc.) were performed on 4 localizers. Maximum errors for Optotrak are most often less than 0.5 mm and 0.1 degrees.[28]] Two rigid bodies consisting of sets of five diodes were used. One rigid body is attached to the robot base and corresponds to the absolute reference. The second rigid body is placed on the end-effector. The 6D relative displacements of these rigid bodies are then recorded.

Mechanical Properties

The aim of this first class of experiments is to observe the behavior of the system under force application. In these two tests, the system is stopped and no computer control is active.

Experiment A: Rigidity

The protocol is as follows:

1. The system is positioned in a configuration where the arm is extended (this is the worst configuration for accumulating the errors); clutching motors are stopped; brakes are active.
2. The initial position of a reference point on the end-effector is recorded.
3. Calibrated forces of 0–3 kg are applied to the end-effector, and 10 positions under force application are recorded for each range of force intensity.

The results are shown in Figure 9. Note that the displacement of the reference point due to the elasticity of the robot may be rather important; up to about 1 cm for forces of 3 kg. This will be discussed later.

Experiment B: Repeatability

This second test aims to determine the ability of the system to return to its initial position after force

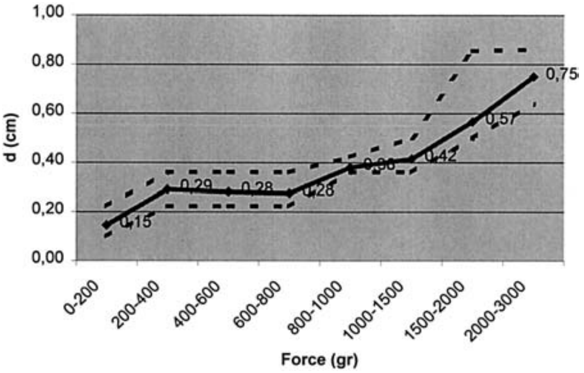

Fig. 9. Force/motion graph: the three curves represent minimum, mean, and maximum values for a given range of force intensity.

application. The protocol is rather similar to the previous one:

1. The system is positioned in a configuration; clutching motors are stopped; brakes are active.
2. The initial position is recorded.
3. Arbitrary forces are applied to the end-effector, and the positions of the reference point (about 100) under force application are recorded.
4. The position after removing the force is recorded.

Position dispersion (step 3) under force application confirms the results of the previous experiments: the position displacement in the vertical direction is very much smaller than in the x and y directions. The effect due to the force application is larger for y than for x because of the selected configuration (arm extended in the x direction). Repeatability is good, as can be seen in Table 1. The repeatability for the x and y axes also differs from that for the z axis.

A third test was conducted in which two rigid bodies were fixed on two successive links of the robot to detect backlash effects in the freewheels. The displacements obtained were too small relative to the Optotrak accuracy to draw conclusions other than that these effects are smaller than the Optotrak accuracy.

Evaluating the Programming Modes

We focused on the accuracy evaluation concerning the position mode for the first five axes and for the sixth translation axis. In these experiments, the axes are computer controlled.

Experiment A: Position Mode—First Five Axes

The protocol is as follows:

1. An arbitrary configuration is selected and recorded (joint variables and Cartesian coordinates of the reference point).
2. The arm is moved far from this initial position to some other arbitrary position.
3. The position mode is used to return to the recorded configuration.
4. The reached position is recorded.
5. Steps 2 to 5 are repeated 10 times.

The results are given in Table 2. The position accuracy is very good. Again, the x, y, and z axes are not equivalent. Mean errors for x, y, and z are respectively 0.53, 0.54, and 0.09 mm. Standard deviations for x, y, and z are, respectively, 0.31, 0.34, and 0.09 mm. These measurements were also used for the evaluation of orientation errors. Roll, pitch, and yaw angles are given in Table 3. These

Table 1. Evaluation of Repeatability after Force Application

	Δx (mm) during force application (100 measurements)		Δy (mm) during force application (100 measurements)		Δz (mm) during force application (100 measurements)	
Test number	Mean	SD	Mean	SD	Mean	SD
1	1.94	1.92	3.47	4.08	0.65	0.55
2	1.44	1.43	1.6	2.18	0.37	0.38
3	1.86	1.65	2.2	1.77	0.61	0.53
4	1.13	0.78	1.08	0.95	0.70	0.52
5	0.95	0.88	2.18	2.37	0.50	0.47

Repeatability (for the five positions)	Δx (mm) after force application	Δy (mm)	Δz (mm)	Δd
Mean	0.38	0.53	0.16	0.70
SD	0.34	0.47	0.18	0.57

SD = Standard deviation.

Table 2. Evaluation of Accuracy in the Position Mode Applied to the First Five Axes

Test number	Δ*x* (mm) after position mode (five axes) (10 measurements) Mean	SD	Δ*y* (mm) after position mode (five axes) (10 measurements) Mean	SD	Δ*z* (mm) after position mode (five axes) (10 measurements) Mean	SD
1	0.52	0.33	0.55	0.41	0.02	0.04
2	0.49	0.32	0.59	0.31	0.08	0.08
3	0.57	0.36	0.47	0.38	0.19	0.07

Global accuracy in the position mode (for the three tests)	Δ*x* (mm)	Δ*y* (mm)	Δ*z*(mm)
Mean	0.53	0.54	0.09
SD	0.31	0.34	0.09

SD = Standard deviation.

orientation errors most probably come from axes 4 and 5. This should be confirmed by further experiments.

Experiment B: Position Mode—Sixth Axis

The protocol consists of the following steps:

1. An arbitrary configuration is selected for the arm; the first five axes are stopped and the brakes are active.
2. A goal position is selected for the needle.
3. The goal position is reached under computer control.
4. The reached position of the needle is recorded.
5. Steps 2 to 5 are repeated 10 times.

The results are given in Table 4. Mean errors for x, y, and z are respectively 0.09, 0.1, and 0.09 mm. Standard deviations for x, y, and z are respectively 0.08, 0.1, and 0.02 mm.

The other modes were tested and are working satisfactorily from the algorithmic point of view. For these other modes, the robot behaves correctly on a qualitative level, even if some tasks may be simpler than others. For example, in the planar region mode, the orientation of the plane in the robot reference frame may lead to a more or less easy interaction with the user. However, no quantitative evaluation has been performed yet; such an evaluation is necessary for further progress with that prototype and its application.

Table 3. Evaluation of Orientation Accuracy in the Position Mode Applied to the First Five Axes

Orientation accuracy in the position mode	Roll error angle (*x* axis)	Pitch error angle (*y* axis)	Yaw error angle (*z* axis)
Mean	0.71	0.76	1
Standard deviation	0.41	0.44	0.51

DISCUSSION

In this paper we have introduced the principle of synergistic systems, described the algorithmic and control issues, and presented a 6DOF PADyC prototype, as well as preliminary experiments performed with this system.

- On a purely algorithmic level, all modes have been successfully tested. Moreover, the system allows for a good interaction with the user when using the different modes. However, as noted previously, a complete quantitative evaluation of the modes is necessary and is planned for the coming months.
- The first set of quantitative tests concerning the two position modes (first five axes and sixth axis) involved in the CASPER application are satisfactory. The different behaviors of the x, y, and z axes are due to the selected architecture. Vertical accuracy is much better than x and y accuracy, but a position can still be reached with very good accuracy that is compatible with the clinical specifications.
- However, concerning the application, two issues have to be discussed. The first is related to robot calibration. In this initial stage of development, we used a simple model of the arm, based on measurements performed by the manufacturer, in which the joints are considered to be perfectly parallel or perpendicular. This model is reasonably accurate. Moreover, the quantitative evaluation we described in the previous section did not require the use of the kinematic model of the arm, and thus

Table 4. Evaluation of Accuracy in the Position Mode Applied to the Sixth Axis

	Δx (mm) after position mode (sixth axis) (10 measurements)		Δy (mm) after position mode (sixth axis) (10 measurements)		Δz (mm) after position mode (sixth axis) (10 measurements)	
Test number	Mean	SD	Mean	SD	Mean	SD
1	0.05	0.05	0.22	0.08	0.09	0.03
2	0.14	0.07	0.06	0.05	0.1	0
3	0.08	0.04	0.04	0.05	0.1	0
Global accuracy in the position mode (for the three tests)	Δx (mm)		Δy (mm)		Δz (mm)	
Mean	0.09		0.1		0.09	
SD	0.08		0.1		0.02	

SD = Standard deviation.

we did not introduce any additional errors because of this simple model. However, further developments will require the selection of a more complex model and the identification of its parameters through calibration procedures. The second issue also concerns accuracy. Modes were tested independently with no cumulative effects. If we consider the puncture application where a position mode for the sixth axis follows a position mode for the first five axes, the orientation accuracy is not so satisfactory. For example, if the first five axes are positioned with an error of 1°, a translation of axis 6 of about 15 cm, which is reasonable for the puncture application, could result in a position error of about 2.5 mm at the target. The reasons for the orientation inaccuracy must be studied carefully, and could lead to some modifications of the mechanical design.

- Experiments also demonstrated that the rigidity of the system is not yet very satisfactory. We can make two remarks on this: first, the tests have been performed in a very unfavorable configuration compared to typical configurations used for the application. Second, the forces used for these experiments were larger than what is typical for clinical actions such as puncturing. However, some other clinical applications that require larger force intensities, such as drilling of bones, could not be executed safely with this current version of PADyC. In light of this, the PADyC structure has to be made more rigid.

Despite some limitations in the present system, the general behaviour of PADyC is very promising, and efforts will be made to ensure its clinical applicability and usability. Several tasks are planned for the future: (a) the quantitative evaluation of the PADyC 6DOF prototype is to be continued; (b) the mechanical behavior of PADyC has to be improved (most likely by miniaturizing the system and redesigning the links) to increase rigidity and reduce orientation errors; and (c) integration with the CASPER application and its evaluation in terms of clinical usability is to be continued.

ACKNOWLEDGMENT

We thank Dr. Olivier Chavanon and Pr. Dominique Blin for their active participation during the clinical specification stage, and the Sinters company for the realization of the prototype.

REFERENCES

1. Mösges R, et al. Computer assisted surgery. An innovative surgical technique in clinical routine. In: Lemke HU, editor: Computer Assisted Radiology (CAR'89). Berlin: Springer-Verlag, 1989. p 413–415.
2. Lavallée S, Sautot P, Troccaz J, Cinquin P, Merloz P. Computer Assisted Spine Surgery: a technique for accurate transpedicular screw fixation using CT data and a 3D optical localizer. In: Proceedings of the First International Symposium on Medical Robotics and Computer Assisted Surgery (MRCAS'94), Pittsburgh, 1994. p 315–322.
3. Grimson W, Ettinger G, White S, Gleason P. Evaluating and validating an automated registration system for enhanced reality visualization in surgery. In: Proceedings of CVRMed'95. Lecture Notes in Computer Science 905. Berlin: Springer, 1995.
4. Taylor RH, et al. A robotic system for cementless total hip replacement surgery in dogs. In: Proceedings of the Second IARP Workshop on Medical and Healthcare Robotics, Newcastle, England, September 1989. p 79–89.
5. Paul H, Bargar W, Mittlestadt B, Musit B, Taylor R, Kazanzides P, Williamson B, Hanson W. Develop-

ment of a surgical robot for cementless total hip arthroplasty. Clin Orthop Rel Res 1992;285:57–66.

6. Lavallée S, et al. Image guided robot: a clinical application in stereotactic neurosurgery. In: Proceedings of the IEEE International Conference on Robotics and Automation, Nice, 1992. p 618–625.
7. Götte H, Roth M, Brack C, Gossé F. A new less-invasive approach to knee surgery using a vision-guided manipulator. In: Proceedings of the IARP Workshop on Medical Robots, Vienna, Austria, 1996. p 99–107.
8. Radermacher K, Staudte HW, Rau G. Computer assisted orthopaedic surgery by means of individual templates—aspects and analysis of potential applications. In: Proceedings of MRCAS'94, Pittsburgh, Pennsylvania. p 42–48.
9. Fortin T, Coudert JL, Champleboux G, Sautot P, Lavallée S. Computer-assisted dental implant surgery using computed tomography. J Image Guid Surg 1995;1:53–58.
10. Guthart GS, Salisbury JK. The Intuitive™ telesurgery system: overview and application. In: Proceedings of the IEEE Robotics and Automation Conference, San Francisco, April 2000.
11. Troccaz J, Peshkin M, Davies B. Guiding systems for Computer-Assisted Surgery (CAS): introducing synergistic devices and discussing the different approaches. Med Image Anal 1998;2(2):101–119.
12. Taylor RH, et al. A model-based optimal planning and execution system with active sensing and passive manipulation for augmentation of human precision in computer-integrated surgery. In: Proceedings of the Second International Conference on Experimental Robotics, Toulouse, France, 1991.
13. Davies B, Harris S, Jakopec M, Cobb J. A novel hands-on robot for knee replacement surgery. In: Proceedings of the Third Annual North American Program on Computer Assisted Orthopaedic Surgery (CAOS USA '99), Pittsburgh, Pennsylvania, June 1999. p 70-74.
14. Harris S, Jakopec M, Cobb J, Davies BL. Intra-operative application of a robotic knee surgery system. In: Taylor C, Colchester A, editors: Proceedings of the Second International Conference on Medical Image Computing and Computer-Assisted Intervention (MICCAI'99), Cambridge, England, September 1999. Lecture Notes in Computer Science 1679. Berlin: Springer, 1999. p 1116–1124.
15. Burghart C, Keitel J, Hassfeld S, Rembold U. Woerm H. Robot controlled osteotomy in craniofacial surgery. In: Proceedings of the 1st International Workshop on Haptic Devices in Medical Applications, Paris, 1999.
16. Davis H, Book W. Torque control of a redundantly actuated passive manipulator. In: Proceedings of the AACC Conference, 1997.
17. Colgate JE, Peshkin M, Moore C. Passive robots and haptic displays based on nonholonomic elements. In: Proceedings of the IEEE International Conference on Robotics and Automation, 1996.
18. Peshkin MA, Colgate JE, Wannasuphoprasi W. Nonholonomic haptic displays. In: Proceedings of the IEEE International Conference on Robotics and Automation, 1996.
19. Troccaz J, Lavallée S, Hellion E. PADyC: a passive arm with dynamic constraints. In: Proceedings of the International Conference on Advanced Robotics (ICAR'93), Tokyo, Japan, 1993. p 361–366.
20. Barraquand J, Latombe JC. Robot motion planning: a distributed representation approach. Technical report STAN-CS-89-1257. Stanford University, Robotics Laboratory, Computer Science Department, 1989.
21. Delnondedieu Y. Un robot à sécurité passive en réponse aux problèmes de sécurité et d'ergonomie en robotique médicale. Ph.D. thesis, Institut National Polytechnique de Grenoble, TIMC laboratory, Grenoble, 1997.
22. Troccaz J, Delnondedieu Y. Synergistic robots for surgery: an algorithmic view of the approach. In: Agarwal P, Kavraki L, Mason M, editors: Robotics: the algorithmic perspective. Proceedings of the Workshop on the Algorithmic Foundations of Robotics (WAFR'98), Houston, 1998. Natick, MS: AK Peters, 1998.
23. Schneider O. Robot à sécurité passive: application à la ponction péricardique. Ph.D. thesis, Institut National Polytechnique de Grenoble, TIMC laboratory, Grenoble, 2001.
24. Troccaz J, Delnondedieu Y. Semi-active guiding systems in surgery. A two-DOF prototype of the passive arm with dynamic constraints (PADyC). Mechatronics 1996;6(4):399–421.
25. Kirkland L, Taylor R. Pericardiocentesis. Crit Care Clin 1992;8:699–712.
26. Chavanon O, Barbe C, Troccaz J, Carrat L, Ribuot C, Blin D. Computer assisted pericardial puncture: work in progress. Comp Aid Surg 1998;2(6):356–364.
27. Chavanon O, Carrat L, Pasqualini C, Dubois E, Blin D, Troccaz J. Computer-guided pericardiocentesis: experimental results and clinical perspectives. Herz 2000;25(8):761–768.
28. Chassat F, Lavallée S. Experimental protocol for accuracy evaluation of 6-D localizers for Computer Integrated Surgery: Application to four optical localizers. In: Wells WM, Colchester A, Delp S, editors: Proceedings of the First International Conference on Medical Image Computing and Computer-Assisted Intervention (MICCAI'98), Cambridge, MA, October 1998. Lecture Notes in Computer Science 1496. Berlin: Springer, 1998. p 277–285.